

Transport approach to anisotropic flows from viscous hydro regime to high p_T

This content has been downloaded from IOPscience. Please scroll down to see the full text.

2013 J. Phys.: Conf. Ser. 446 012025

(<http://iopscience.iop.org/1742-6596/446/1/012025>)

View [the table of contents for this issue](#), or go to the [journal homepage](#) for more

Download details:

IP Address: 191.179.76.122

This content was downloaded on 26/06/2016 at 07:03

Please note that [terms and conditions apply](#).

Transport approach to anisotropic flows from viscous hydro regime to high p_T

Salvatore Plumari^{1,2}, Armando Puglisi², Francesco Scardina^{1,2} and Vincenzo Greco^{1,2}

¹ Department of Physics and Astronomy, University of Catania, Via S. Sofia 64, I-95125 Catania (Italy)

² Laboratorio Nazionale del Sud, INFN-LNS, Via S. Sofia 63, I-95125 Catania (Italy)

E-mail: salvatore.plumari@hotmail.it

Abstract. We discuss the build up of the elliptic flow v_2 in a transport approach at fixed viscosity. We point out that in the intermediate transverse momentum region flows are also sensitive to microscopic details of the cross section, while hydrodynamics suffers from large uncertainties due to the non-equilibrium correction to the distribution function. We show, exploring the temperature dependence of η/s , that a study of v_2 in a wide p_T range allows to understand the difference behind the collective flows at LHC respect to RHIC. In particular the transport approach provides a tool able to naturally describe the rise and fall and saturation of the $v_2(p_T)$.

1. Introduction

In recent years the experimental results accumulated in the ultra relativistic heavy ion collisions before at RHIC program at BNL and more recently at the LHC program at CERN has shown that the elliptic flow v_2 is the largest ever seen in Heavy Ion Collision (HIC) [1, 2]. Viscous hydrodynamics at second order in gradient expansion according to the Israel-Stewart theory [3, 4, 5] is the most commonly used framework to describe the evolution of the fireball created in these collisions. Here all the information is encoded in a few macroscopic parameter like the Equation of State and shear viscosity. The comparison between the experimentally measured v_2 and theoretical calculations have suggested that an almost perfect fluid with a very small shear viscosity to entropy density ratio η/s has been created, with a viscosity of the order of $4\pi\eta/s \approx 1 - 3$ [3, 5]. Similar conclusions have been obtained from kinetic transport theory [6, 7, 8]. Hydrodynamics however has the fundamental problem of a limited range of validity in η/s and in the transverse momentum $p_T \leq 2$ GeV. At increasing p_T the validity of viscous hydrodynamics breaks because the relative deviation from the equilibrium distribution function $\delta f/f_{eq}$ increases with p_T becoming large already at $p_T \geq 3T \sim 1$ GeV. Due to the sensitivity of the elliptic flow on the ratio η/s it becomes important to know the correct relation between $\eta \leftrightarrow T, \sigma(\theta)$. In literature there are several approximation methods for the calculation of η one of these is the Chappmann-Enskog (CE) [9]. In Ref.[10] it has been shown that CE supplies an analytical expression for η with an accuracy better than 5% while the Relaxation Time Approximation (RTA) underestimates η by a factor 2 and therefore it provides a way to construct a kinetic theory at fixed $\eta/s(T)$. In this proceeding we will show some results for v_2



in the framework of a parton cascade at fixed η/s with a larger accuracy with respect to first tentatives in RTA [7, 4, 8].

2. The parton cascade at fixed η/s

Our approach is a 3 + 1 dimensional Monte Carlo cascade [7] for on-shell partons based on the stochastic interpretation of the collision rate [11]. In the following discussion we use the pQCD inspired cross section typically used in parton cascade approaches [6, 7, 11, 12, 13]:

$$\frac{d\sigma}{dt} = \frac{9\pi\alpha_s^2}{2} \frac{1}{(t - m_D^2)^2} \left(1 + \frac{m_D^2}{s}\right) \quad (1)$$

where s, t are the Mandelstam variables and m_D is the Debye thermal mass. In the CE approximation the shear viscosity assumes the following form $\eta = g(z, T/m_D) \frac{T}{\sigma_{tot}}$ (see [10]), where σ_{tot} is the total cross section while $g(z, T/m_D)$ is given by the following expression

$$g(z, \bar{a})^{-1} = \frac{8}{5} \frac{z}{K_3^2(z)} \int_1^\infty dy (y^2 - 1)^3 h(2^{-1} z^{-2} y^{-2} \bar{a}^2) \left[(z^2 y^2 + 1/3) K_3(2zy) - zy K_2(2zy) \right] \quad (2)$$

Where the function h is related to the transport cross section $\sigma_{tr} = \sigma_{tot} h(a)$ with $h(a) = 4a(1+a)[(2a+1)\ln(1+1/a) - 2]$ while $a = m_D^2/s$ and $\bar{a} = m_D/T$. In our approach we solve the relativistic Boltzmann equation with the constraint that η/s is fixed during the dynamics of the collisions in a way similar to [14] but with an exact local implementation as described in detail in [7]. We evaluate locally in space and time the strength of the cross section $\sigma_{tot}(\rho, T)$ needed to have η/s at the wanted value. Therefore considering that the entropy density for a massless gas is $s = \rho(4 - \mu/T)$ with μ being the fugacity, the total cross section assume the following expression $\sigma_{tot} = \frac{g(m_D, T)}{\rho(4 - \mu/T)} \frac{T}{\eta/s}$. Within this approach the total cross section has the form $\sigma_{tot} = K(\rho, T) \sigma_{pQCD} > \sigma_{pQCD}$ where $K(\rho, T)$ takes into account the non perturbative effects responsible to keep fixed the ratio η/s . Note that this approach has been shown to recover the viscous hydrodynamics evolution of the bulk system [4, 7], but implicitly assume that also high p_T particles collide with largely nonperturbative cross section [15, 16]. Within this approach the kinetic freeze out is given by the increase of η/s at lower temperature, see red solid line in Fig.2. This naturally realizes a freeze out (f.o.) because it implies a smooth reduction of σ_{tot} .

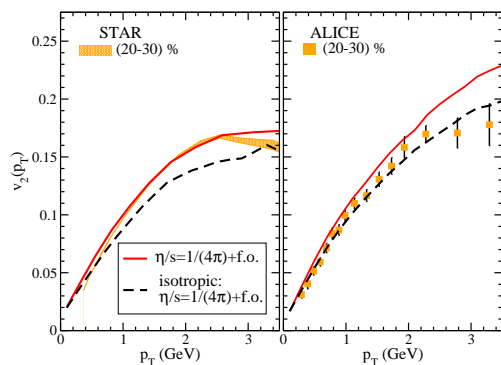


Figure 1. $v_2(p_T)$ at mid rapidity for 20% – 30% collision centrality for RHIC (left panel) and LHC (right panel), data taken by [2]. The red solid line is the calculation with $4\pi\eta/s = 1$ and the inclusion of freeze out (f.o.) and with an anisotropic cross section with finite m_D while the black dashed line is the case with an isotropic cross section ($m_D \rightarrow \infty$).

3. Elliptic flow within a parton cascade at fixed η/s

In our calculation the initial conditions are longitudinal boost invariant. We have assumed parton-hadron duality and the initial $dN/d\eta$ has been chosen in order to reproduce the final

$dN_{ch}/d\eta(b)$ at mid rapidity observed in the experiments at RHIC and LHC energies. The initial condition in coordinate space are given by the Glauber model. In the momentum space at RHIC (LHC) the partons with $p_T \leq p_0 = 2$ GeV (4 GeV) are distributed according to a thermalized spectrum with a maximum temperature in the center of the fireball of $T_0 = 2T_C$ ($T_0 = 3T_C$) while for $p_T > p_0$ we take the spectrum of non-quenched minijets according to standard NLO-pQCD calculations. The initial time is $t_0 = 0.6$ fm/c at RHIC and $t_0 = 0.3$ fm/c at LHC. As shown in Fig.1 in the low p_T region ($p_T < 1.5$ GeV) the v_2 depends on the value of η/s while for higher value of p_T the v_2 becomes an observable sensitive to the microscopical details of the interaction (namely on the value of m_D). For the case shown in the figure with the increase of the thermal debye mass (toward an isotropic cross section), we observe a suppression of the v_2 . In order to study the role of η/s in the build up of v_2 we have considered in our simulations three different temperature dependences for η/s , with a constant $4\pi\eta/s = 1$ during all the evolution of the system (black dashed line), with a constant $4\pi\eta/s = 1$ in the QGP phase but with freeze out (f.o.) (red solid line) and finally the case with f.o. and $4\pi\eta/s \propto T^2$ in the QGP phase (blue dot-dashed line), see Fig.2. As shown in Fig. 3, the $\eta/s(T)$ affects the generation of the v_2 in different way between RHIC and LHC. This different behaviour of v_2 can be explained looking at the different life time of the fireball between RHIC and LHC. The life time of the fireball is smaller at RHIC than that at LHC energies, 4 – 5 fm/c at RHIC against the about 8 – 10 fm/c at LHC. Therefore the elliptic flow at RHIC has not enough time to develop completely and it becomes more sensitive to the value of η/s in the cross over region (for $T \approx T_C$) while at LHC due to a larger life time the v_2 can develop completely and it can discriminate better the value of η/s in the QGP phase. The comparison with data would suggest that at LHC they are compatible with a linear T-increase of η/s . Similar calculations performed in the framework of viscous hydrodynamics (see Ref.[17]) have shown a good description of the data for almost central collisions with a slightly stronger temperature dependence of η/s than that used in our work. As pointed out in [15, 16] the procedure discussed in the previous section doesn't permit

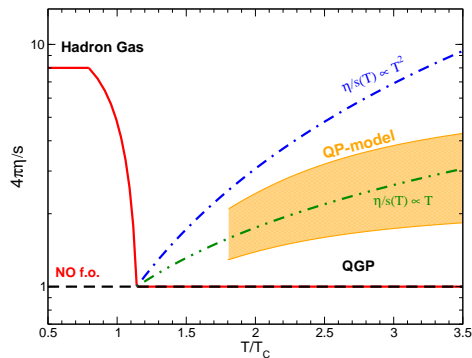


Figure 2. Different temperature dependent parametrizations for η/s . The orange area take into account the quasi-particle model predictions for η/s [18]. The solid, dashed and dot dashed lines are the three different temperature profiles of $\eta/s(T)$ used in our simulations, see Fig.3.

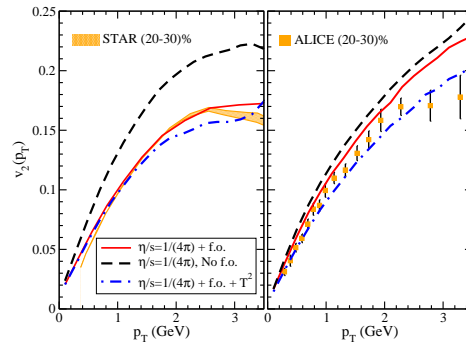


Figure 3. $v_2(p_T)$ for 20% – 30% collision centrality for RHIC (left panel) and LHC (right panel), data taken by [2]. The black dashed lines is the case with $4\pi\eta/s = 1$ and without f.o., the red line is the case with $4\pi\eta/s = 1$ with f.o. while the blue dot-dashed line refers to the case with f.o. and $4\pi\eta/s \propto T^2$ in the QGP phase.

to recover the pQCD limit for hard collision therefore a natural way to extend it is to consider a K factor that depends on the invariant energy of the collision $K(s)$. This is a way to switch off non-perturbative effects at higher s . We have chosen for $K(s)$ the following exponential

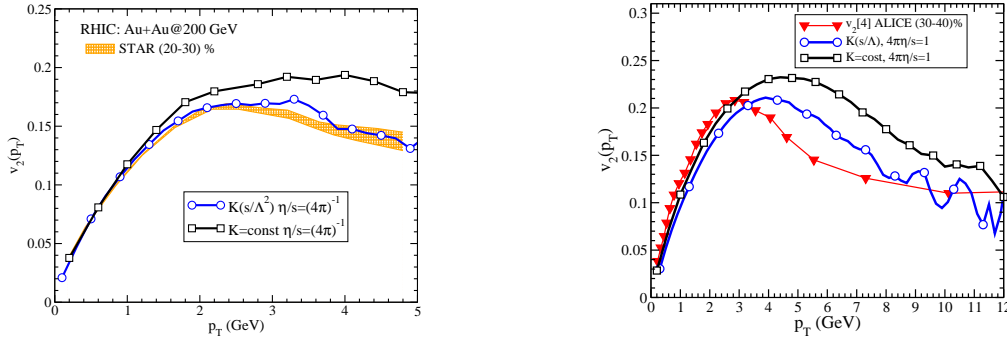


Figure 4. $v_2(p_T)$ for 20% – 30% collision centrality for RHIC (left) and LHC (right) with $4\pi\eta/s = 1$ and f.o., data taken by [2]. The black lines with squares are the cases with $K = const$ while the blue lines with circles are the same calculations but with $K(s/\Lambda)$ with $\Lambda = 3$ GeV.

form $K(s/\Lambda^2) = 1 + \gamma e^{-s/\Lambda^2}$, where Λ is a scale parameter that fix the energy scale for the transition to pQCD behaviour (where $K(s) \rightarrow 1$). While γ plays the same role of K in the old calculations and it is determined again in order to keep fixed locally the η/s . In Fig.4 we have shown the results for the v_2 obtained using the RTA for the viscosity [15]. The implementation with the CE parametrization is in progress. A comparison between RHIC and LHC shows that the effect of the $K(s/\Lambda^2)$ function is to reduce the v_2 at high p_T for both energies. In general with the inclusion of $K(s/\Lambda^2)$ we can reproduce the shape of the elliptic flow as shown in the experiments in a very wide range of p_T . We can interpret the raise of v_2 as an effect due to the non perturbative behaviour at low p_T while the fall and consequently saturation as given by the disappearance of the non perturbative effect and the restoration of the pQCD behavior.

4. Conclusions

We have investigated within a parton cascade approach the effect of a temperature dependent η/s on the generation of v_2 at RHIC and LHC. Our calculations show that the v_2 at RHIC is sensitive to the f.o. (hadronic phase) while at LHC all the v_2 comes from the QGP phase and the hadronic phase is irrelevant on it. Furthermore we observe that the v_2 in the intermediate p_T region becomes an observable sensitive to the microscopical details of the system.

References

- [1] Adams J *et al.* (STAR Collaboration) 2005 *Nucl.Phys.* **A757** 102–183 (*Preprint nucl-ex/0501009*)
- [2] Aamodt K *et al.* (ALICE Collaboration) 2010 *Phys.Rev.Lett.* **105** 252302 (*Preprint 1011.3914*)
- [3] Romatschke P and Romatschke U 2007 *Phys.Rev.Lett.* **99** 172301 (*Preprint 0706.1522*)
- [4] Huovinen P and Molnar D 2009 *Phys.Rev.* **C79** 014906 (*Preprint 0808.0953*)
- [5] Song H and Heinz U W 2008 *Phys.Rev.* **C78** 024902 (*Preprint 0805.1756*)
- [6] Xu Z and Greiner C 2009 *Phys.Rev.* **C79** 014904 (*Preprint 0811.2940*)
- [7] Ferini G, Colonna M, Di Toro M and Greco V 2009 *Phys.Lett.* **B670** 325–329 (*Preprint 0805.4814*)
- [8] Plumari S, Baran V, Di Toro M, Ferini G and Greco V 2010 *Phys.Lett.* **B689** 18–22 (*Preprint 1001.2736*)
- [9] Wiranata A and Prakash M 2012 *Phys.Rev.* **C85** 054908 (*Preprint 1203.0281*)
- [10] Plumari S, Puglisi A, Scardina F and Greco V 2012 *Phys.Rev.* **C86** 054902 (*Preprint 1208.0481*)
- [11] Xu Z and Greiner C 2005 *Phys.Rev.* **C71** 064901 (*Preprint hep-ph/0406278*)
- [12] Plumari S, Baran V, Di Toro M and Greco V 2011 *J.Phys.Conf.Ser.* **270** 012061 (*Preprint 1009.2664*)
- [13] Molnar D and Gyulassy M 2002 *Nucl.Phys.* **A697** 495–520 (*Preprint nucl-th/0104073*)
- [14] Molnar D 2008 (*Preprint 0806.0026*)
- [15] Plumari S and Greco V 2012 *AIP Conf.Proc.* **1422** 56–61 (*Preprint 1110.2383*)
- [16] Plumari S, Puglisi A, Colonna M, Scardina F and Greco V 2012 (*Preprint 1209.0601*)
- [17] Niemi H, Denicol G, Huovinen P, Molnar E and Rischke D 2012 *Phys.Rev.* **C86** 014909 (*Preprint 1203.2452*)
- [18] Plumari S, Alberico W M, Greco V and Ratti C 2011 *Phys.Rev.* **D84** 094004 (*Preprint 1103.5611*)